Published in final edited form as:
J Neurosci Methods. 2014 December 30; 238: 95–104. doi:10.1016/j.jneumeth.2014.09.013.

An explant muscle model to examine the refinement of the synaptic landscape

Martin Gartz Hanson and **Lee A. Niswander**
Howard Hughes Medical Institute, Dept. of Pediatrics, University of Colorado School of Medicine and Children's Hospital Colorado, Aurora, CO 80045

Abstract

Signals from nerve and muscle regulate the formation of synapses. Transgenic mouse models and muscle cell cultures have elucidated the molecular mechanisms required for aggregation and stabilization of synaptic structures. However, far less is known about the molecular pathways involved in redistribution of muscle synaptic components. Here we established a physiologically viable whole-muscle embryonic explant system, in the presence or absence of the nerve, which demonstrates the synaptic landscape is dynamic and malleable. Manipulations of factors intrinsic to the muscle or extrinsically provided by the nerve illustrate vital functions during formation, redistribution and elimination of acetylcholine receptor (AChR) clusters. In particular, RyR1 activity is an important mediator of these functions. This physiologically relevant and readily accessible explant system provides a new approach to genetically uncouple nerve-derived signals and for manipulation via signaling molecules, drugs, and electrical stimulation to examine early formation of the neuromuscular circuit.

Keywords

Acetylcholine receptor; neuromuscular junction; synapse formation; muscle fiber; agrin; neuregulin

1. Introduction

In the nervous system, patterns of electrical activity induce pre-synaptic molecular mechanisms involved in axon guidance and fine-tuning of connections to target tissues (Hanson and Landmesser, 2006, 2004; Hubel and Wiesel, 1962). The motor axon connection with the muscle results in the formation of large synapses, known as neuromuscular junctions (NMJ), and the postsynaptic NMJ in postnatal animals has been well studied. During embryogenesis and development of the axon-muscle connection, the

Corresponding author: M. Gartz Hanson; University of Colorado School of Medicine; Bldg. L18-12400; 12801 E. 17th Ave., Aurora, CO 80045, martin.hanson@ucdenver.edu, Phone: 303 724-3794, FAX: 303 724-3792.

Conflict of Interest: The authors declare that no conflict of interest exists.

muscle assembles the synaptic components that will eventually comprise the NMJ postsynaptic apparatus. The main synaptic components assembled and clustered in the embryonic muscle are acetylcholine receptors (AChR). Transgenic studies provide evidence that AChR clusters can assemble independently of the nerve (Lin et al., 2001). Axons of the phrenic nerve innervate the mouse diaphragm at embryonic day 13.5 (E13.5). As the nerve grows on the muscle at E14.5, aneural AChR clusters distribute near but not directly apposed to the nerve (Lin et al., 2001), which has been called “prepatterning” (Figure 1a) (Lin et al., 2001; Lomo, 2003; Witzemann, 2006; Yang et al., 2001). After E16.5, AChR clusters are juxtaposed to the nerve (Lin et al., 2001). The change of AChR clusters from broad prepattern to redistribution at the nerve endplates suggests that the embryonic nerve influences the organization of AChR clusters (Misgeld et al., 2002). Communication from the nerve onto the muscle induces muscle-intrinsic pathways that function in redistribution of AChR clusters (Brandon et al., 2003; Lin et al., 2005; Misgeld et al., 2002; Misgeld et al., 2005; Pacifici et al., 2011) and elimination of non-innervated AChR clusters (Lin et al., 2005; Misgeld et al., 2005; Wang et al., 2014). Motor axons release acetylcholine (ACh), which depolarizes muscle and disperses AChRs, whereas Agrin stimulates MuSK and stabilizes AChRs (Lin et al., 2005; Misgeld et al., 2005). Muscle cell cultures have revealed several mechanisms that regulate the assembly, formation and elimination of aneural AChR clusters. A limitation of myotube cultures is that they do not become differentiated muscle fibers and AChR clusters are not regionalized or patterned within the myotube cultures. Additional insights have come from mouse mutants that show defects in prepatterning and redistribution of AChR clusters (Lin et al., 2001; Lin et al., 2005; Misgeld et al., 2005). However, because the mammalian embryo develops in utero, the manner in which these defects arise has been difficult to evaluate by snap-shots in time. Studies of changes in the synaptic landscape would be significantly enhanced by methodology to experimentally manipulate the system and observe the outcome over time. Here we developed a mouse embryonic diaphragm explant culture system to examine formation, elimination and redistribution of the prepatterned AChR clusters. This provides a new approach to probe the transformations within the synaptic landscape and its molecular control.

2. Materials and Methods

2.1 Mice

Richard Allen generated the *RyR1*^{tm1TAlle} (*dyspedic)* mice. *Mnx1*$^{tm4(cre)Tmj}$ (*Mnx1*^{null}) was purchased through JAX. B6.Cg-Tg(Hlxb9-GFP)1Tmj/J was purchased through JAX to label the phrenic nerve. All mice were bred at least 5 generations into 129SvJ background. Homozygous null *RyR1*^{null} and *Mnx1*^{null} embryos were obtained by timed pregnancies of heterozygous matings; noon of the day when a vaginal plug was detected was designated as embryonic (E) day 0.5. After selected intervals of in utero development, null embryos and their littermate controls were collected from pregnant mice. All experimental protocols followed NIH Guidelines and were approved by the University of Colorado Institutional Animal Care and Use Committee.

2.2 Diaphragm muscle explant

The E15.5 muscle explant system is similar to adult explants of the murine triangularis sterni (Kerschensteiner et al., 2008). E15.5 embryos were dissected in oxygenated Tyrode's Solution and pinned to a dish with a layer of Sylgard (184, Dow Corning) and the skin removed to expose the ribcage. A portion of the ribcage surrounding the diaphragm (last 5–8 caudal ribs) was removed from the embryo with a small scissors and placed with the rostral surface up on another 100mM Sylgard coated dish and the ribcage slightly stretched and pinned down using insect pins. The dish was placed in a 30°C heated chamber with perfused oxygenated (95% O_2/5% CO_2) Tyrode's Solution.

The xenonerve preparation is modified from (Hanson and Landmesser, 2003). E15.5 embryos, in which the phrenic nerve was GFP-positive, had their cortex ablated. The spinal cord and hindbrain were exposed through removal of the cranium and dorsal spinal column. All internal organs were removed. The phrenic nerve was carefully dissected from the lungs, arteries and ribcage under a flow of oxygenated Tyrode's Solution. The GFP-positive phrenic nerve was detached from the diaphragm and pinned to isolated *Mnx1*^{null} diaphragms. The xenonerve explant was pinned above the isolated *Mnx1*^{null} diaphragm in order to allow contact of the xenonerve nerve to the isolated diaphragm.

Electrical stimulation of the diaphragm by field potential electrode (STG 1002 stimulator) induced contraction of wildtype muscle. A 200ms stimulation pulse was induced every 3 or 10 minutes for 8 hours in a 30 °C bath of perfused Tyrode's solution.

2.3 Immunohistochemistry

Diaphragms were dissected and pinned to Sylgard dish in 4% paraformaldehyde for 10 min then permeabilized with 0.2% Triton/PBS for 30 min. Non-specific reactivity was blocked with 3% BSA/PBS for 2 hours. Diaphragms were incubated overnight at 4 degrees in 0.3% triton-x, 3% BSA, AChR clusters were labeled with α-bungarotoxin conjugated 488 (1:500; Invitrogen) and nerves visualized with monoclonal antibody to Neurofilament M (160 kD) conjugated to DY547 (1:500; Abcam). Samples were examined on a confocal laser scanning microscopy Zeiss LSM 510 META.

2.4 Quantification of AChR cluster number

The method of quantification of AChR receptor cluster number was a modification to Kim and Burden (Kim and Burden, 2008). AChR cluster number was quantified on compressed z-stack images of entire muscle at 0.1 mm bins from the central branch in right ventral quadrant outlined by blue boxes in Figure 4i. In Kim and Burden (2008) quantification was performed using total pixel intensity per bin. However, this method was difficult to reproduce due to wildtype, *Mnx1*^{null}, and *Ryr1*^{null} showing different size AChR clusters (unpublished observation). Therefore, each AChR cluster was counted within the 0.1 mm bins. The ventral quadrant shows a high degree of reproducibility in axon branching, AChR cluster number and distribution. In *Ryr1*^{null} diaphragms, phrenic nerve branches that normally innervate the dorsal crus muscle would occasionally grow through the dorsal quadrant of the diaphragm with several AChR clusters expressed under the this central region of the nerve branch (unpublished observation). Thus, the dorsal quadrant was

excluded in all experiments. Each condition was performed on at least 5 diaphragms for each condition.

2.5 Quantification of AChR cluster region

Drawing a line between the most distal α-bungarotoxin positive AChR clusters and measuring the distance in ~10μm intervals on each side of the central branch nerve in the ventral diaphragm quadrant quantified AChR cluster region. To determine the percent of the region occupied by AChR clusters, the distance to the distal edges of the diaphragm and the region of α-bungarotoxin labeled AChR clusters was measured in 100μm increments. Percentage of AChR clusters was quantified using compressed z-stack images. Each condition was performed in at least 5 diaphragms for each condition.

2.6 Statistical Analysis

The unpaired two-tailed Student's t test was used to compare means for statistical differences. Data in the manuscript are represented as mean ± SEM unless otherwise indicated. $P < 0.05$ was considered significant.

3. Results

3.1 Viable diaphragm explants show malleability of AChR clustering

The mouse embryonic diaphragm is a model for the study of synapse formation due to its stereotypical pattern of innervation along the central region of the muscle. The purpose of this study was to create an explant system using the intact diaphragm muscle, with or without the nerve, to study the dynamics of, and mechanisms underlying, elimination, redistribution, and induction of new AChR clusters following their initial prepatterned clustering. We focused our attention on E15.5 mouse diaphragms, in which phrenic nerve outgrowth on the muscle has concluded but AChR clusters are not yet juxtaposed to the phrenic nerve (Figure 1b)(Lin et al., 2001). Diaphragms still connected to the rib cage were dissected at a time of prepatterned clusters (E15.5) and cultured as explants, which can survive for over 8 hours at 30°C in perfused Normal Tyrode's solution. To create a diaphragm lacking the nerve, we used the *Mnx1*^{null} allele (also known as *Hb9* or *Hlxb9*)(Lin et al., 2001). Over 16 hours of culture, the AChR cluster distribution looked similar between explants and freshly dissected diaphragms without a nerve (Figure 1d, i–k compared to Figure 1c). To determine the influence of the nerve on AChR cluster redistribution, a fluorescently labeled phrenic nerve (xenonerve with attached CNS from E15.5 *Mnx1*$^{GFP/+}$ embryo, see methods) was pinned to the central region of the *Mnx1*^{null} diaphragm muscle (Figure 1f) and the explant cultured. The xenonerve could narrow the pattern of AChR clusters after 8 hours of culture (Figure 1e, i; the nerve is not seen in Figure 1e as it is pinned above the diaphragm preparation) in contrast to littermate controls lacking the phrenic nerve and without the xenonerve (Figure 1d, i; yellow vertical line on the left of figure panels represents AChR cluster distribution in the figure shown). Interestingly, nerve-dependent redistribution of the AChR clusters occurred several hundred microns away from the xenonerve in the perfused bath solution suggesting that signals from the nerve can induce redistribution of AChR cluster at a distance. AChR clusters redistributed to the central region, in accordance with the concentration of AChR transcripts in this region (Lin et al.,

2001). Thus, transmission of nerve-derived signals and not axon outgrowth pattern can dictate the placement of the AChR clusters.

Neurotransmission of ACh drives depolarization and voltage dependent release of internal calcium stores. The voltage of the action potential travels through the t-tubule conduits to depolarize the dihydropyridine receptor (DHPR, $Ca_V1.1$), which mechanically opens ryanodine receptor type 1 (RyR1) channels in the sarcoplasmic reticulum (SR). RyR1 channels release intracellular calcium stores to flood the myofiber with calcium, which initiates muscle contraction, known as excitation-contraction (E-C) coupling, to permit locomotion (Beam and Franzini-Armstrong, 1997; Takeshima et al., 1994). As shown above, nerve-dependent signals are required for AChR cluster redistribution. This data suggests that ACh neurotransmission through molecular and/or electrical signaling might be required for AChR redistribution. AChR redistribution has been investigated in muscle cell cultures but depolarization experiments are difficult to implement because the cells often detach from the dish as they undergo contraction. Moreover, the junction between the t-tubule and SR is not fully functional in myotubes compared to differentiated muscle fibers. Thus, we next determined whether muscle depolarization is sufficient to refine and redistribute the pattern of AChR clusters using explants of diaphragms lacking a nerve.. *Mnx1*^{null} diaphragms were electrically stimulated with a field potential stimulation at a frequency of one pulse every three minutes (5.6mHz) or ten minutes (1.7mHz) for >6 hours to induce muscle contractions. Depolarization of the muscle was capable of narrowing the pattern of AChR clusters (Figure 1g–i). Moreover, stimulated diaphragms showed a decrease in the number of AChR clusters (Table 1). These data imply that muscle intrinsic patterning process can render the future post-synaptic density zone independent of Agrin signaling of MuSK, while destabilizing AChR clusters independent of ACh release by the nerve.

3.2 Activity dependent Wnt3a elimination of AChR clusters

While electrical activity and nerve contact can refine the pattern of AChR clusters, muscle-derived signals additionally refine the pattern of AChR clusters (Lin et al., 2001; Stamatakou and Salinas, 2013). In myotube cultures, elimination of AChR clusters can transpire through Wnt3a, which suppresses signaling required for AChR formation (Wang et al., 2008). Moreover in myotube cultures, ACh-dependent caspase-3 cleavage of Dishevelled, a Wnt signaling protein, induces elimination of postsynaptic structures (Wang et al., 2014). However, we found that bath application of Wnt3a (30ng/ml) did not significantly decrease the number or distribution of AChR clusters in wildtype or *Mnx1*^{null} diaphragms (Figure 2a,b and 2c compared to Figure 1i, Table 1). Based on our stimulation data, muscle electrical activity can induce AChR cluster redistribution and elimination. Two types of depolarization, focal and global, take place in muscle during the stimulation protocol. The focal depolarization is the local activation of AChR by ACh, while the global depolarization is the large action potential that travels throughout the t-tubule network to produce E-C coupling. The manner of depolarization that induces declustering is unclear and hence we used the explant system to attempt to define whether global depolarization is important in AChR cluster elimination.

Two mouse models which disrupt E-C coupling show disorganization of AChR clusters: targeted deletion of β1 subunit of DHPR *(Cacnb1^{null}*) which significantly increases *Musk* RNA expression and drastically increases spontaneous ACh-dependent depolarizing events (Chen et al., 2011) and deletion of Stac3 (Nelson et al., 2013), which disrupts the voltage activation of DHPR and causes broad depolarization. To determine whether there is a relationship between DHPR activity and Wnt3a signaling to affect AChR number and/or distribution, nitrendipine (10μM), an antagonist of DHPR, was applied with Wnt3a to *Mnx1^{null}* diaphragms. Within 4 hours, ~50% of the AChR clusters were eliminated, and ~72% were eliminated within 6 hours, and those that remained were distributed to the central region (Figure 2c–f, Table 1, Figure 3). This data suggests that DHPR activity inhibits Wnt3a function, possibly through Dishevelled (Wang et al., 2014), to control AChR cluster elimination. This data combined with the findings of Chen (2011) would suggest that functional DHPR could repress both elimination and assembly of AChR clusters.

3.3 RyR1 is required for distribution of AChR clusters

The voltage sensitive L-type calcium channel DHPR is mechanically linked with RyR1 to induce calcium release and E-C coupling during an action potential. Therefore, the antagonistic affect of nitrendipine on DHPR would also inhibit the actions of RyR1. To test the applicability of the explant system to both genetic and experimental manipulation, we generated mouse embryos that lacked RyR1 activity (*Ryr1^{tm1Alle}* (Buck et al., 1997), referred to as *Ryr1^{null}*) and lacked nerves (*Mnx1^{null}*) and treated these diaphragm explants with Wnt3a. Wnt3a, applied to *Ryr1^{null}* or *Ryr1^{null}*; *Mnx1^{null}* diaphragm explants, significantly decreased the number of AChR clusters (Figure 2g–i), suggesting that inhibition of DHPR and the mechanically linked RyR1 might be required for Wnt3a mediated AChR elimination in aneural regions of the diaphragm.

The elimination of AChR clusters by Wnt3a in *Ryr1^{null}* diaphragm explants suggests that RyR1 activity could be involved in the organization of AChR clusters during embryonic development. In *Ryr1^{null}* diaphragms at both E15.5 and E18.5, AChR clusters were directly adjacent to the main nerve bundle resulting in a significantly narrower pattern (Figure 4b, f, j, k) compared to wildtype diaphragms (Figure 4a, e, j, k). In the absence of the phrenic nerve (*Mnx1^{null}*) but in the presence of RyR1 activity (*Ryr1^{WT}*), AChR clusters were scattered in the broader prepatterned distribution (Figure 4c, g, j, k). However, in the absence of RyR1 function and absence of phrenic nerve (*Ryr1^{null}*; *Mnx1^{null}*), the AChR clusters were spread well beyond the prepatterned region (Figure 4d, h, j, k). Thus, in the absence of RyR1 function, the nerve influences the pattern of AChR clusters, whereas in the absence of both RyR1 and nerve, AChR clusters distribute throughout the diaphragm (compare Figure 4b, f with d, h). To experimentally test whether muscle electrical activity-induced refinement of AChR clustering requires RyR1 function, we again turned to the explant system. Depolarization (5.6mHz stimulation) in the absence of both RyR1 and phrenic nerve eliminated most AChR clusters (Figure 5d, e compared to Figure 5b, c, Table 1) yet the remaining AChR clusters were randomly distributed throughout the diaphragm explant (Figure 5d, f), thus demonstrating that RyR1 is required for the AChR cluster redistribution during depolarization. These data suggest that both muscle and nerve

components determine AChR cluster positioning, and that RyR1-dependent muscle activity or nerve contact are sufficient to redistribute AChR clusters.

3.4 Exploration of extrinsic factors in diaphragm explants

During contact with the muscle, the nerve produces two extrinsic factors that control the aggregation and stabilization of AChR clusters: Agrin and Neuregulin-1 (NRG1). In myotube cultures, Agrin aggregates ACh receptors, counteracts the inhibitory affect of ACh on synapse formation, prevents caspase-3 dispersion of AChR clusters and stabilizes AChR clusters (Misgeld et al., 2005; Reist et al., 1992; Rimer, 2010; Wang et al., 2014), while NRG1 inhibits AChR aggregation by Agrin (Trinidad and Cohen, 2004). Constitutive expression of ErbB2, the receptor for NRG1 inhibits Agrin induced AChR clusters in myotubes and induces synaptic loss when expressed *in vivo* (Ponomareva et al., 2006). More recently, NRG1/ErbB2 signaling was shown to maintain high efficacy of synaptic transmission by stabilizing the postsynaptic apparatus in adult muscle (Schmidt et al., 2011). We addressed whether extrinsic factors showed comparable properties in diaphragm-explant cultures compared to myotube cultures. In diaphragm explants, application of NRG1 (0.1 ng/ml) did not significantly affect overall number of AChR clusters in nerve innervated explants (Table 1) but in the absence of the nerve, NRG1 treatment produced centralized redistribution and reduced numbers of the AChR clusters, with or without RyR1 activity (Figure 5g–i compare with Figure 5a, b; Table 1), suggesting that NRG1 is involved in the redistribution of AChR clusters to the central region of the E15.5 embryonic diaphragm.

In embryonic diaphragms, neuronal-released Agrin is involved in stability of juxtaposed AChR clusters; however, Agrin is not implicated in AChR cluster prepatterning (Lin et al., 2001; Misgeld et al., 2005; Reist et al., 1992; Rimer, 2010; Wang et al., 2014). Agrin treatment (5 ng/ml) of wild type explants with or without the nerve did not induce new AChR clusters (Table 1; Figure 5j, l). In *RyR1*^{null} diaphragms with the phrenic nerve, AChR clusters were significantly increased adjacent to the nerve by Agrin treatment (Table 1). Without the phrenic nerve in *RyR1*^{null} diaphragms, Agrin increased the number of AChR clusters and expanded their distribution to the full extent of the diaphragm (Table 1 and Figure 5k, l compared to Figure 5b, c). These data suggest that RyR1 activity represses Agrin-induced AChR clusters. Thus, RyR1 activity plays a dual role to control elimination of aneural AChR clusters by Wnt3a and to control aggregation of AChR clusters by Agrin.

3.5 Exploration of an intrinsic signaling mechanism in diaphragm explants

As shown above, RyR1 activity influences extrinsic factor activity during AChR cluster distribution. To explore further the usefulness of the diaphragm explant system, we next examined intrinsic mechanistic pathways linked to AChR cluster redistribution. Protein Kinase A (PKA) targets and activates RyR1 (Reiken et al., 2003; Suko et al., 1993). Moreover, PKA activity causes phosphorylation and activation of the NRG1 receptor, ErbB2, in the muscle (Monje et al., 2008). PKA phosphorylates AChR and increases the number of AChR clusters in myotube cultures (Lanuza et al., 2006; Li et al., 2001). In the diaphragm explant system, the PKA activator, 6-Benz cAMP (100μM), induced redistribution of AChR clusters in the absence of the nerve, such that the pattern became more similar to that of treated innervated muscle, with no change in AChR cluster number

(Figure 6a–c; Table 1). As an additional test, the explants were cultured in 8-CPT-2′-O-Me cAMP (100μM), an agonist of the exchange proteins that activate cAMP (EPAC) but which have no effect on ErbB2 function. CPT-2′-O-Me cAMP had no effect on AChR redistribution and a modest effect on AChR cluster number (Figure 6d–f; Table 1), emphasizing the importance of NRG1 in AChR redistribution. PKA is also a known regulator of CDK5 function (Liu et al., 2006). In innervated *Cdk5*^{null} diaphragms, AChR clusters are directly adjacent to the nerve and the axons sprout beyond the AChR clusters, similar to *Ryr1*^{null} diaphragms (Fu et al., 2005) (Figure 4f). CDK5 activity is inhibited by roscovitine (Lin et al., 2005). Roscovitine (100μM) caused AChR clusters to spread beyond the prepatterned region with no change in AChR cluster number (Figure 6g–i; Table 1). These data suggest that NRG1 and RyR1 induce redistribution of prepatterned AChR clusters via PKA activation. Moreover, these data suggest an involvement of CDK5 function in the distribution of AChR clusters.

4. Discussion

The embryonic diaphragm explant system provides a new model to explore the malleability of AChR clusters. This physiologically intact system can be used to genetically uncouple nerve-derived signals and it allows access for manipulation via signaling molecules, drugs, and electrical stimulation. Using this innovative whole muscle explant system we have provided several important insights into the dynamics of AChR cluster prepatterning and the mechanisms underlying the distribution of AChRs. First, the propensity of Wnt3a to eliminate aneural AChRs is sensitive to RyR1 activity and DHPR activity. Second, RyR1 counteracts the ability of Agrin to aggregate AChR clusters. Third, as with the case of E-C coupling proteins DHPR and Stac3 (Chen et al., 2011; Nelson et al., 2013), RyR1 is required for proper distribution of aneural and neuronal AChR clusters. Finally, we provide mechanistic evidence that PKA and CDK5 are molecular players within the muscle that control regionalization of aneural AChR clusters.

Components of AChR cluster maintenance and elimination are focally controlled by motor nerve release of ACh and Agrin as well as signaling through Dishevelled (Misgeld et al., 2005; Reist et al., 1992; Rimer, 2010; Wang et al., 2014). The role of NRG1 in AChR clustering is less clear. Patterns of AchR clustering and synapse formation are normal in mice lacking Neuregulin or its receptors (Escher et al., 2005; Jaworski and Burden, 2006; Yang et al., 2001). In myotube cultures that lack axons, NRG1 inhibits AChR aggregation by Agrin (Trinidad and Cohen, 2004). Constitutive expression of ErbB2, the receptor for NRG1, inhibits Agrin induced AChR clusters in myotubes and induces synaptic loss when expressed *in vivo* (Ponomareva et al., 2006). In adult muscle, NRG1/ErbB2 signaling stabilizes the postsynaptic apparatus (Schmidt et al., 2011). In our explant preparation, NRG1 redistributes AChR clusters to a more centralized region of the muscle. Our data may suggest that NRG1 signaling is playing a dual role. In non-centralized regions of muscle, NRG1 may destabilize AChR clusters. In centralized regions, NRG1 may stabilize AChR clusters. These data in muscle explants that lack nerves suggest that muscle intrinsic mechanism help determine the distribution of AChR clusters.

These data lead to a broader question of how the synaptic landscape is dynamically shaped by E-C coupling machinery. We postulate that within the muscle, DHPR-RyR1 global activity transpires during the early stages of nerve-muscle contact and AChR clustering. The mechanism by which DHPR and RyR1 oversee the patterning of AChR clusters in the presence of the nerve is likely independent of their roles in E-C coupling, as the pattern of AChR clusters in diaphragms null for the beta subunit of DHPR (*Cacnb1*^{null}) are distributed throughout the diaphragm with axon overgrowth (Chen et al., 2011) while the AChR clusters are narrowed near the phrenic nerve in *RyR1*^{null} diaphragms. In the absence of the nerve, the mechanism by which DHPR and RyR1 oversee prepatterning is likely reliant on their roles in E-C coupling, as the pattern of AChR clusters in *RyR1*^{null}/*Mnx1*^{null} and *Cacnb1*^{null}/*Mnx1*^{null} diaphragms (Chen et al., 2011) are comparably spread throughout the diaphragm beyond the prepatterned region. Interestingly, in the absence of nerve-derived action potentials, RyR1 channels are active and induce Ca^{2+} efflux from internal stores (Armstrong et al., 1972; Schneider and Ward, 2002).

Moreover, pharmacological inhibition of DHPR activity or genetic loss of *RyR1*^{null} shows similar elimination of AChR clusters in the presence of Wnt3a in our prepatterning model. Our data demonstrates that Agrin signaling induces ectopic AChR cluster formation in E15.5 diaphragms that lack RyR1 activity. Following a muscle contraction, intracellular calcium and sodium are rapidly increased and subsequently decreased to inhibit contractions (Allen et al., 1984; Deitmer and Ellis, 1978; Eisner et al., 1983). We theorize that the local and transient inhibition of voltage dependent E-C coupling may allow Agrin-dependent stabilization of nerve-juxtaposed AChR clusters and Wnt3a elimination of aneural AChR clusters. Together, multiple mechanisms within the muscle are involved in determining the expression and position of AChR clusters. In the future, this intact explant system will be useful in determining the role of neurotransmitter receptor clustering in synaptic physiology, in assessing nerve-muscle interactions during embryonic development, and in mouse modeling of congenital disorders.

Acknowledgments

We thank Lori Bulwith and Rosa Moreno for experimental guidance and technical assistance, Kurt Beam for the *RyR1*^{null} mice, and Matt Lee and U.J. McMahan for comments on the manuscript. This work was supported by postdoctoral fellowships from MDA69338 and NIH F32 NS059267 (MGH). LN is an investigator of the Howard Hughes Medical Institute.

References

Allen DG, Eisner DA, Orchard CH. Factors influencing free intracellular calcium concentration in quiescent ferret ventricular muscle. J Physiol. 1984; 350:615–30. [PubMed: 6747860]

Armstrong CM, Bezanilla FM, Horowicz P. Twitches in the presence of ethylene glycol bis(-aminoethyl ether)-N,N′-tetracetic acid. Biochim Biophys Acta. 1972; 267:605–8. [PubMed: 4537984]

Beam KG, Franzini-Armstrong C. Functional and structural approaches to the study of excitation-contraction coupling. Methods Cell Biol. 1997; 52:283–306. [PubMed: 9379955]

Brandon EP, Lin W, D'Amour KA, Pizzo DP, Dominguez B, Sugiura Y, Thode S, Ko CP, Thal LJ, Gage FH, Lee KF. Aberrant patterning of neuromuscular synapses in choline acetyltransferase-deficient mice. J Neurosci. 2003; 23:539–49. [PubMed: 12533614]

Buck ED, Nguyen HT, Pessah IN, Allen PD. Dyspedic mouse skeletal muscle expresses major elements of the triadic junction but lacks detectable ryanodine receptor protein and function. J Biol Chem. 1997; 272:7360–7. [PubMed: 9054435]

Chen F, Liu Y, Sugiura Y, Allen PD, Gregg RG, Lin W. Neuromuscular synaptic patterning requires the function of skeletal muscle dihydropyridine receptors. Nat Neurosci. 2011; 14:570–7. [PubMed: 21441923]

Deitmer JW, Ellis D. Changes in the intracellular sodium activity of sheep heart Purkinje fibres produced by calcium and other divalent cations. J Physiol. 1978; 277:437–53. [PubMed: 650551]

Eisner DA, Lederer WJ, Vaughan-Jones RD. The control of tonic tension by membrane potential and intracellular sodium activity in the sheep cardiac Purkinje fibre. J Physiol. 1983; 335:723–43. [PubMed: 6875898]

Escher P, Lacazette E, Courtet M, Blindenbacher A, Landmann L, Bezakova G, Lloyd KC, Mueller U, Brenner HR. Synapses form in skeletal muscles lacking neuregulin receptors. Science. 2005; 308:1920–3. [PubMed: 15976301]

Fu AK, Ip FC, Fu WY, Cheung J, Wang JH, Yung WH, Ip NY. Aberrant motor axon projection, acetylcholine receptor clustering, and neurotransmission in cyclin-dependent kinase 5 null mice. Proc Natl Acad Sci U S A. 2005; 102:15224–9. [PubMed: 16203963]

Hanson MG, Landmesser LT. Characterization of the circuits that generate spontaneous episodes of activity in the early embryonic mouse spinal cord. J Neurosci. 2003; 23:587–600. [PubMed: 12533619]

Hanson MG, Landmesser LT. Increasing the frequency of spontaneous rhythmic activity disrupts pool-specific axon fasciculation and pathfinding of embryonic spinal motoneurons. J Neurosci. 2006; 26:12769–80. [PubMed: 17151280]

Hanson MG, Landmesser LT. Normal patterns of spontaneous activity are required for correct motor axon guidance and the expression of specific guidance molecules. Neuron. 2004; 43:687–701. [PubMed: 15339650]

Hubel DH, Wiesel TN. Receptive fields, binocular interaction and functional architecture in the cat's visual cortex. J Physiol. 1962; 160:106–54. [PubMed: 14449617]

Jaworski A, Burden SJ. Neuromuscular synapse formation in mice lacking motor neuron- and skeletal muscle-derived Neuregulin-1. J Neurosci. 2006; 26:655–61. [PubMed: 16407563]

Kerschensteiner M, Reuter MS, Lichtman JW, Misgeld T. Ex vivo imaging of motor axon dynamics in murine triangularis sterni explants. Nat Protoc. 2008; 3:1645–53. [PubMed: 18833201]

Kim N, Burden SJ. MuSK controls where motor axons grow and form synapses. Nat Neurosci. 2008; 11:19–27. [PubMed: 18084289]

Lanuza MA, Gizaw R, Viloria A, Gonzalez CM, Besalduch N, Dunlap V, Tomas J, Nelson PG. Phosphorylation of the nicotinic acetylcholine receptor in myotube-cholinergic neuron cocultures. J Neurosci Res. 2006; 83:1407–14. [PubMed: 16555299]

Li MX, Jia M, Jiang H, Dunlap V, Nelson PG. Opposing actions of protein kinase A and C mediate Hebbian synaptic plasticity. Nat Neurosci. 2001; 4:871–2. [PubMed: 11528415]

Lin W, Burgess RW, Dominguez B, Pfaff SL, Sanes JR, Lee KF. Distinct roles of nerve and muscle in postsynaptic differentiation of the neuromuscular synapse. Nature. 2001; 410:1057–64. [PubMed: 11323662]

Lin W, Dominguez B, Yang J, Aryal P, Brandon EP, Gage FH, Lee KF. Neurotransmitter acetylcholine negatively regulates neuromuscular synapse formation by a Cdk5-dependent mechanism. Neuron. 2005; 46:569–79. [PubMed: 15944126]

Liu F, Liang Z, Shi J, Yin D, El-Akkad E, Grundke-Iqbal I, Iqbal K, Gong CX. PKA modulates GSK-3beta- and cdk5-catalyzed phosphorylation of tau in site- and kinase-specific manners. FEBS Lett. 2006; 580:6269–74. [PubMed: 17078951]

Lomo T. What controls the position, number, size, and distribution of neuromuscular junctions on rat muscle fibers? J Neurocytol. 2003; 32:835–48. [PubMed: 15034271]

Misgeld T, Burgess RW, Lewis RM, Cunningham JM, Lichtman JW, Sanes JR. Roles of neurotransmitter in synapse formation: development of neuromuscular junctions lacking choline acetyltransferase. Neuron. 2002; 36:635–48. [PubMed: 12441053]

Misgeld T, Kummer TT, Lichtman JW, Sanes JR. Agrin promotes synaptic differentiation by counteracting an inhibitory effect of neurotransmitter. Proc Natl Acad Sci U S A. 2005; 102:11088–93. [PubMed: 16043708]

Monje PV, Athauda G, Wood PM. Protein kinase A-mediated gating of neuregulin-dependent ErbB2-ErbB3 activation underlies the synergistic action of cAMP on Schwann cell proliferation. J Biol Chem. 2008; 283:34087–100. [PubMed: 18799465]

Nelson BR, Wu F, Liu Y, Anderson DM, McAnally J, Lin W, Cannon SC, Bassel-Duby R, Olson EN. Skeletal muscle-specific T-tubule protein STAC3 mediates voltage-induced Ca2+ release and contractility. Proc Natl Acad Sci U S A. 2013; 110:11881–6. [PubMed: 23818578]

Pacifici PG, Peter C, Yampolsky P, Koenen M, McArdle JJ, Witzemann V. Novel mouse model reveals distinct activity-dependent and -independent contributions to synapse development. PLoS One. 2011; 6:e16469. [PubMed: 21305030]

Ponomareva ON, Ma H, Vock VM, Ellerton EL, Moody SE, Dakour R, Chodosh LA, Rimer M. Defective neuromuscular synaptogenesis in mice expressing constitutively active ErbB2 in skeletal muscle fibers. Mol Cell Neurosci. 2006; 31:334–45. [PubMed: 16278083]

Reiken S, Lacampagne A, Zhou H, Kherani A, Lehnart SE, Ward C, Huang F, Gaburjakova M, Gaburjakova J, Rosemblit N, Warren MS, He KL, Yi GH, Wang J, Burkhoff D, Vassort G, Marks AR. PKA phosphorylation activates the calcium release channel (ryanodine receptor) in skeletal muscle: defective regulation in heart failure. J Cell Biol. 2003; 160:919–28. [PubMed: 12629052]

Reist NE, Werle MJ, McMahan UJ. Agrin released by motor neurons induces the aggregation of acetylcholine receptors at neuromuscular junctions. Neuron. 1992; 8:865–8. [PubMed: 1316763]

Rimer M. Modulation of agrin-induced acetylcholine receptor clustering by extracellular signal-regulated kinases 1 and 2 in cultured myotubes. J Biol Chem. 2010; 285:32370–7. [PubMed: 20696763]

Schmidt N, Akaaboune M, Gajendran N, Martinez-Pena y Valenzuela I, Wakefield S, Thurnheer R, Brenner HR. Neuregulin/ErbB regulate neuromuscular junction development by phosphorylation of alpha-dystrobrevin. J Cell Biol. 2011; 195:1171–84. [PubMed: 22184199]

Schneider MF, Ward CW. Initiation and termination of calcium sparks in skeletal muscle. Front Biosci. 2002; 7:d1212–22. [PubMed: 11991854]

Stamatakou E, Salinas PC. Postsynaptic assembly: A role for Wnt signaling. Dev Neurobiol. 2013

Suko J, Maurer-Fogy I, Plank B, Bertel O, Wyskovsky W, Hohenegger M, Hellmann G. Phosphorylation of serine 2843 in ryanodine receptor-calcium release channel of skeletal muscle by cAMP-, cGMP- and CaM-dependent protein kinase. Biochim Biophys Acta. 1993; 1175:193–206. [PubMed: 8380342]

Takeshima H, Nishi M, Iwabe N, Miyata T, Hosoya T, Masai I, Hotta Y. Isolation and characterization of a gene for a ryanodine receptor/calcium release channel in Drosophila melanogaster. FEBS Lett. 1994; 337:81–7. [PubMed: 8276118]

Trinidad JC, Cohen JB. Neuregulin inhibits acetylcholine receptor aggregation in myotubes. J Biol Chem. 2004; 279:31622–8. [PubMed: 15155732]

Wang J, Ruan NJ, Qian L, Lei WL, Chen F, Luo ZG. Wnt/beta-catenin signaling suppresses Rapsyn expression and inhibits acetylcholine receptor clustering at the neuromuscular junction. J Biol Chem. 2008; 283:21668–75. [PubMed: 18541538]

Wang JY, Chen F, Fu XQ, Ding CS, Zhou L, Zhang XH, Luo ZG. Caspase-3 cleavage of dishevelled induces elimination of postsynaptic structures. Dev Cell. 2014; 28:670–84. [PubMed: 24631402]

Witzemann V. Development of the neuromuscular junction. Cell Tissue Res. 2006; 326:263–71. [PubMed: 16819627]

Yang X, Arber S, William C, Li L, Tanabe Y, Jessell TM, Birchmeier C, Burden SJ. Patterning of muscle acetylcholine receptor gene expression in the absence of motor innervation. Neuron. 2001; 30:399–410. [PubMed: 11395002]

Highlights

- Use of innovative whole muscle explant system examining the dynamics of AChR cluster prepatterning.
- RyR1 activity and DHPR activity repress Wnt3a ability to eliminate aneural AChRs.
- RyR1 counteracts the ability of Agrin to aggregate AChR clusters.
- RyR1 is required for proper distribution of aneural and neuronal AChR clusters.
- PKA and CDK5 are molecular players within the muscle that control regionalization of aneural AChR clusters.

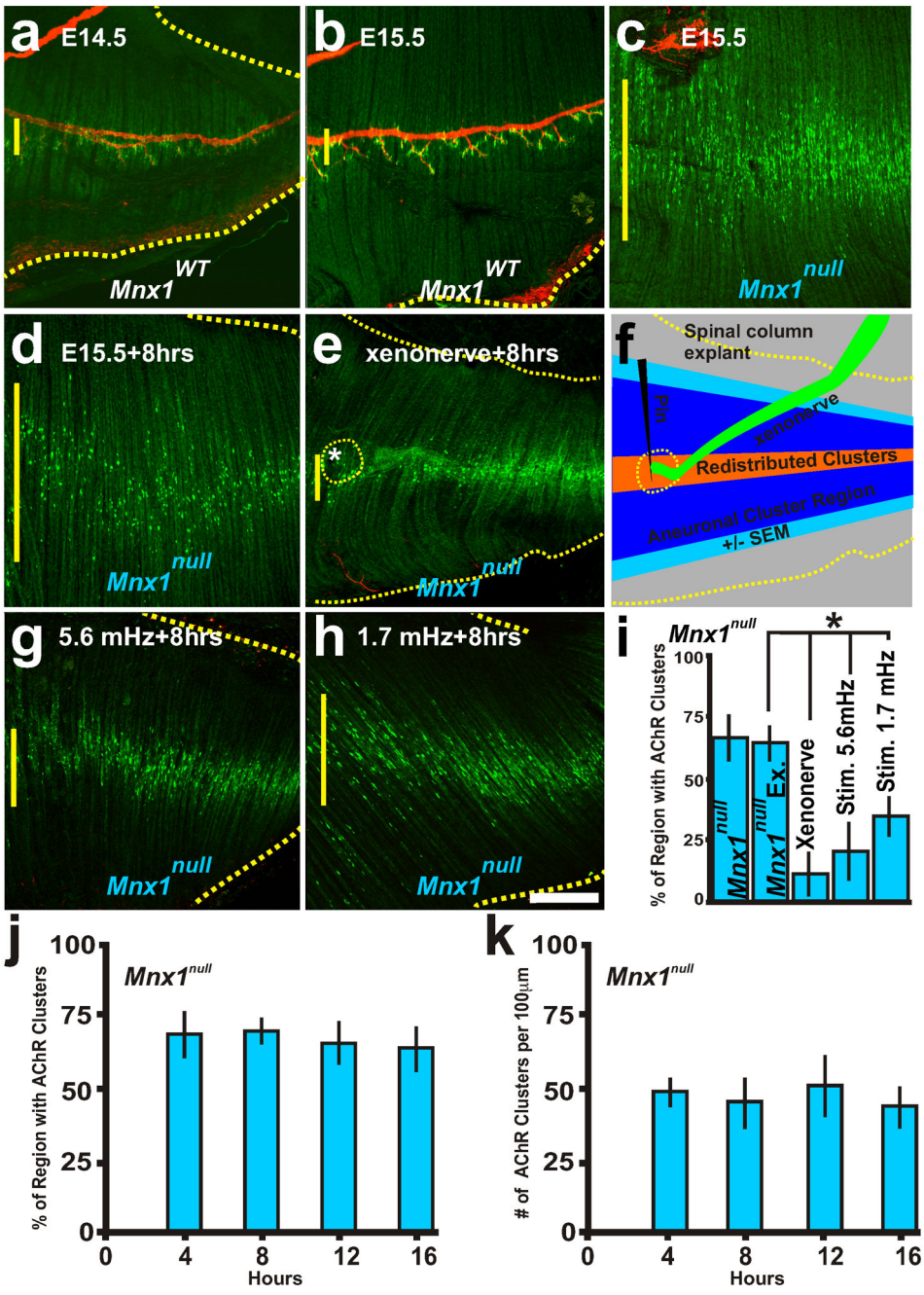

Figure 1.

Neuronal and electrical activity cues control the distribution of AChR clusters. Representative examples of AChR clusters (α-bungarotoxin conjugated Alexa-488; green) and the phrenic nerve (neurofilament-160; red). **a, b,** E14.5 and E15.5 diaphragm from wildtype mice with AChR clusters apposed to the phrenic nerve. **c,** E15.5 diaphragms from *Mnx1*^{null} mice without a phrenic nerve. **d,** E15.5 *Mnx1*^{null} diaphragm explant cultured for 8 hours. **e,** Littermate *Mnx1*^{null} diaphragm with *Mnx1*$^{GFP/+}$ spinal cord-phrenic nerve explant pinned during 8 hr culture (asterisk and dotted yellow line indicate xenonerve placement, the xenonerve detached during fixation) shows a narrowed AChR cluster region compared to **d.**

f, Schematic of explant showing the region of aneural AChR clusters at the start of the experiment (blue) and the redistribution and centralization of AChR clusters in the presence of the xenonerve (orange). **g, h,** E15.5 *Mnx1*^{null} diaphragms stimulated every 3 minutes (5.6 mHz) or 10 minutes (1.7 mHz) for 8 hours induces redistribution and elimination of AChR clusters. **i,** Quantification of the distribution of AChR clusters within the *Mnx1*^{null} explant diaphragms before and after culture, with xenonerve, and following electrical stimulation. **j, k,** Percent regionalization (**j)** and number (**k)** of AChR clusters at 4, 8, 12, and 16 hours of culture of *Mnx1*^{null} diaphragm explants. Scale bar = 200 μm; yellow vertical line on the left of each panel represents the largest width of the AChR cluster region within ventral quadrant of diaphragm shown. Each condition was examined in 5 diaphragms.

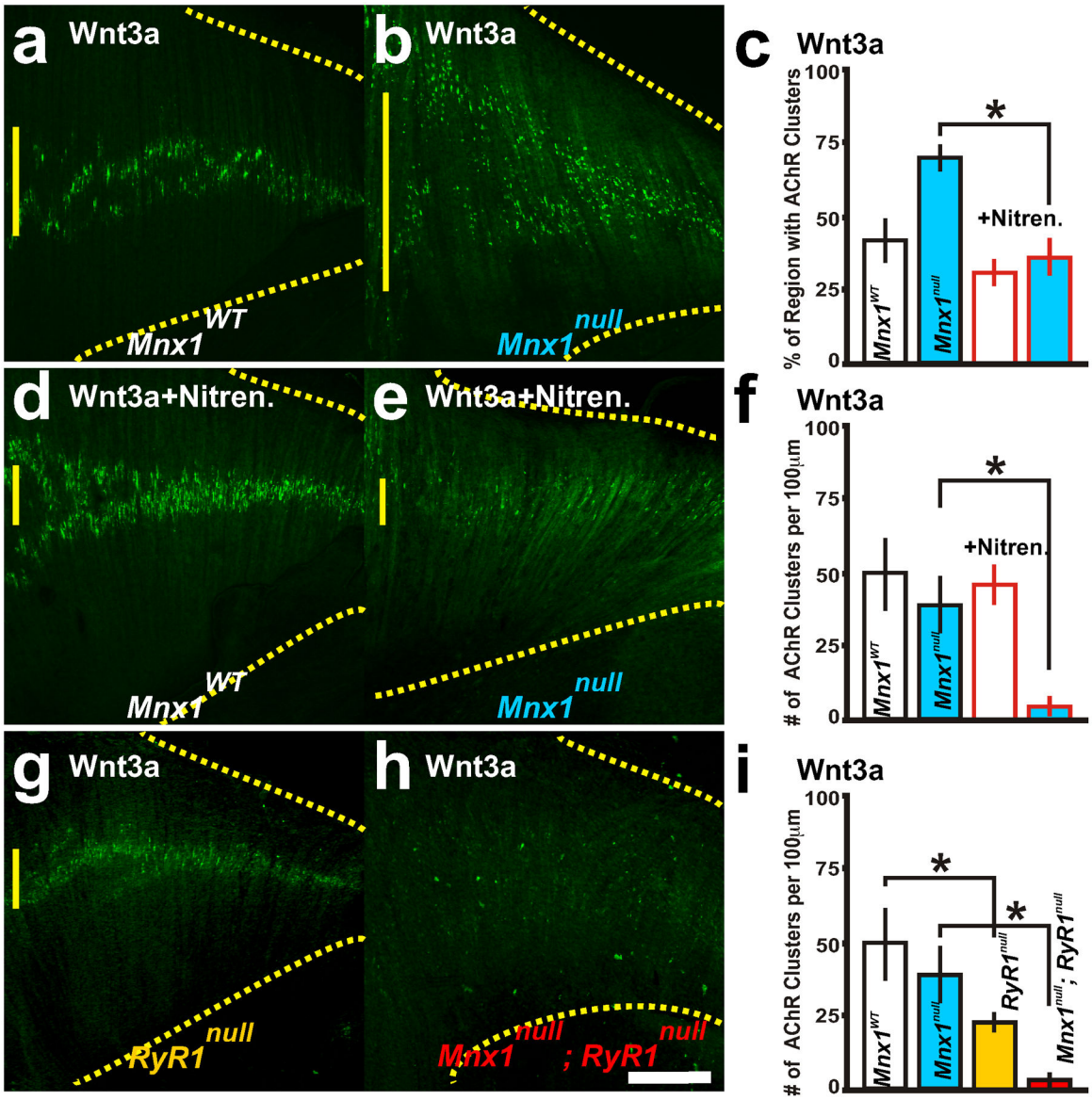

Figure 2.

Wnt3a induces AChR cluster elimination when DHPR and RyR1 function is inhibited. **a–i,** Wnt3a (30ng/ml) treated diaphragm explants with α-bungarotoxin labeled AChR clusters. **a–f,** Wildtype (**a, d**) and *Mnx1*^{null} (**b, e**) littermate diaphragm explants treated in Wnt3a without (**a, b**) and with 10μM nitrendipine, an antagonist to DHPR channels (**d, e**; red outlined bars in **c, f**). Percent regionalization (**c**) and number (**f**) of AChR clusters. *RyR1*$^{-/-}$ (**g**) and *RyR1*$^{-/-}$*; Mnx1*^{null} (**h**) explants treated with Wnt3a. **i, N**umber of AChR clusters. Asterisks show significance ($p<0.005$) of samples compared to control explants. Scale bar = 200 μm; yellow vertical line on the left of each panel represents the largest width of the AChR cluster region within ventral quadrant of diaphragm shown. Each condition was performed in 5 diaphragms.

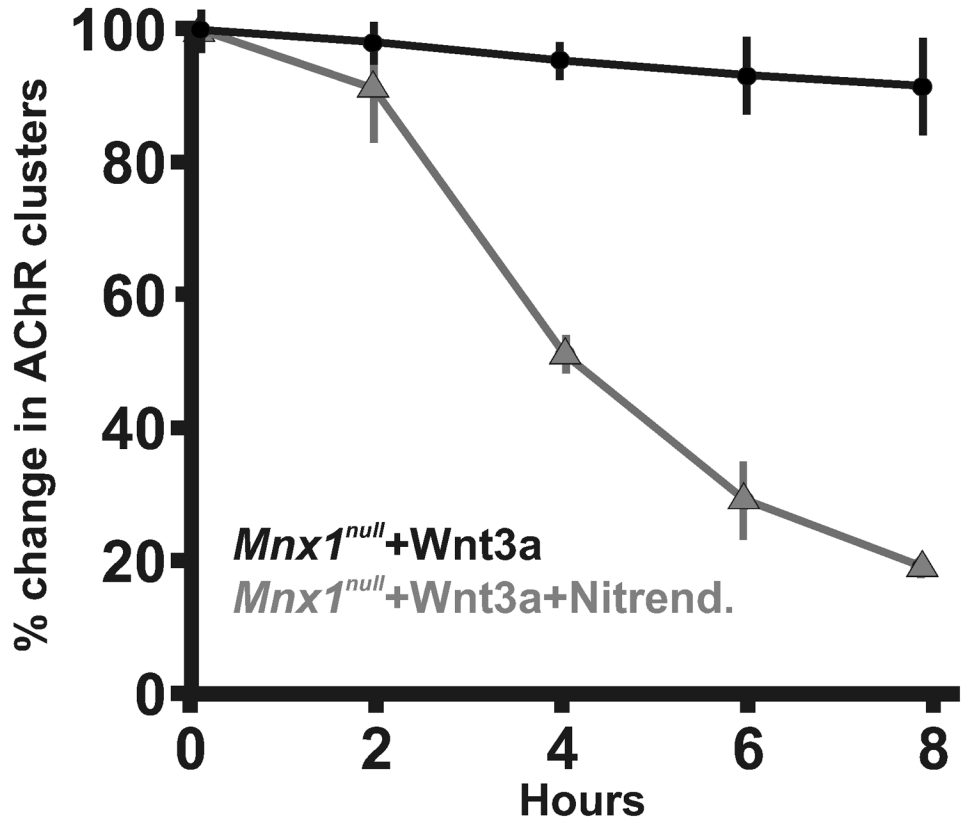

Figure 3.

Percent change in AChR clusters over time in explant diaphragms that lack phrenic nerves (*Mnx1*^{null}) and treated with Wnt3a (black circles) or treated with Wnt3a and nitrendipine, an antagonist to DHPR channels (grey triangles). Each condition was performed in 5 diaphragms.

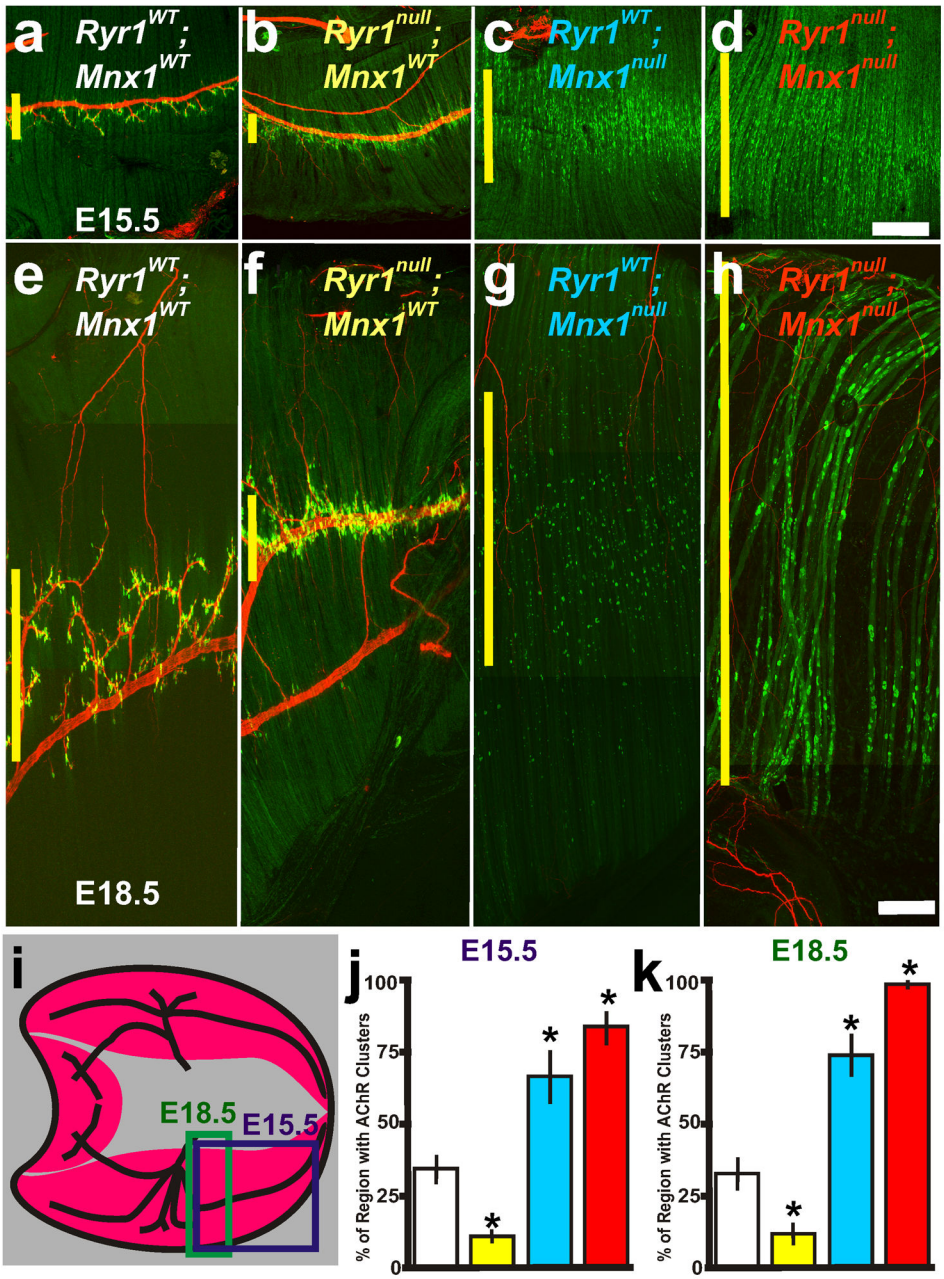

Figure 4.

Nerve and muscle components are required for centralization of AChR clusters. **a–d**, E15.5 and **e–h**, E18.5 composite pictures of diaphragm muscle from *RyR1*^{WT}; *Mnx1*^{WT} (white lettering and box in **j,k**), *RyR1*^{null}; *Mnx1*^{WT} (yellow), *RyR1*^{WT}; *Mnx1*^{null} (blue) and *RyR1*^{null}; *Mnx1*^{null} (red). **i,** Illustration of diaphragm muscle and regions analyzed at E15.5 (purple box) and E18.5 (green rectangle representation of composite picture in **f)**. Purple rectangle represents E15.5 images and regions of quantification presented in figure graphs at E15.5. **j**, E15.5 graph of the percent of diaphragm with patterned AChR clusters in all diaphragm crosses examined in **ad. k**, E18.5 graph of the percent of diaphragm with patterned AChR clusters in all diaphragm crosses examined in **e–h** excluding random AChR clusters in

RyR1^{null}; *Mnx1*^{WT} diaphragm muscles (n=5 per cross). Asterisks show significance ($p<0.05$) of samples compared to control. Scale bar for **a–d**=200μm; for **e–h**= 50 μm. **a, c** are from Figure 1b,c. Yellow vertical line on the left of each panel represents the largest width of the AChR cluster region within ventral quadrant of diaphragm shown. Each condition was performed in 6 diaphragms.

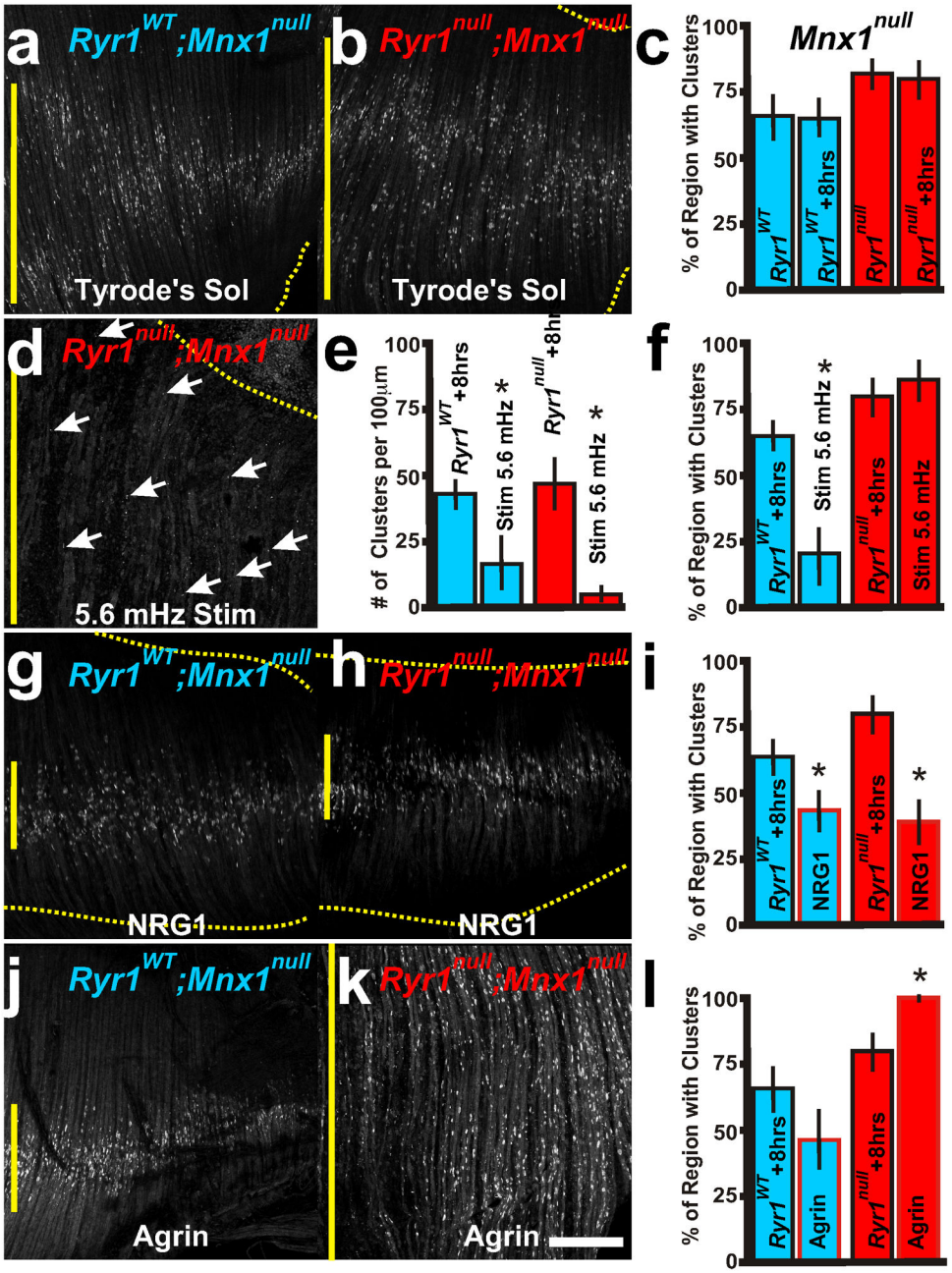

Figure 5.

Extrinsic factors that affect redistribution of AChR clusters. Representative examples of E15.5 *RyR1*^{WT}*; Mnx1*^{null} (**a, g, j**, blue lettering and boxes in graphs) and *RyR1*^{null}; *Mnx1*^{null} (**b, d, h, k**, red) diaphragm AChR clusters (α-bungarotoxin) after explant culture. **c, f, i, l,** Quantification of regionalization in various 8 hour explant treatments. **d–f**, *RyR1*^{null}*; Mnx1*^{null} explant that was stimulated every 3 minutes for 8hr (5.6 mHz) does not centralize AChR clusters (white arrows, red box in **e** compared to *RyR1*^{WT}*; Mnx1*^{null}, blue box) and there are fewer AChR clusters (**f**). **g–i,** Neuregulin (NRG1) treated explant cultures (red outlined boxes in **i**) show narrowing of AChR clusters in both genetic samples. **j–l,** Agrin

treatment (red outlined boxes in **l**) increases AChR cluster formation and distribution in *RyR1*^{null}; *Mnx1*^{null} (**k, l**) explants yet does not increase AChR formation in *RyR1*^{WT} *Mnx1*^{null} **(j, l)** explants. Asterisks show significance ($p<0.05$) of samples compared to explant controls of *RyR1*^{WT} and *RyR1*^{null}. Scale bar = 200 μm; yellow vertical line represents the largest width of the AChR cluster region within ventral quadrant of diaphragm shown. Each condition was performed in 5 diaphragms.

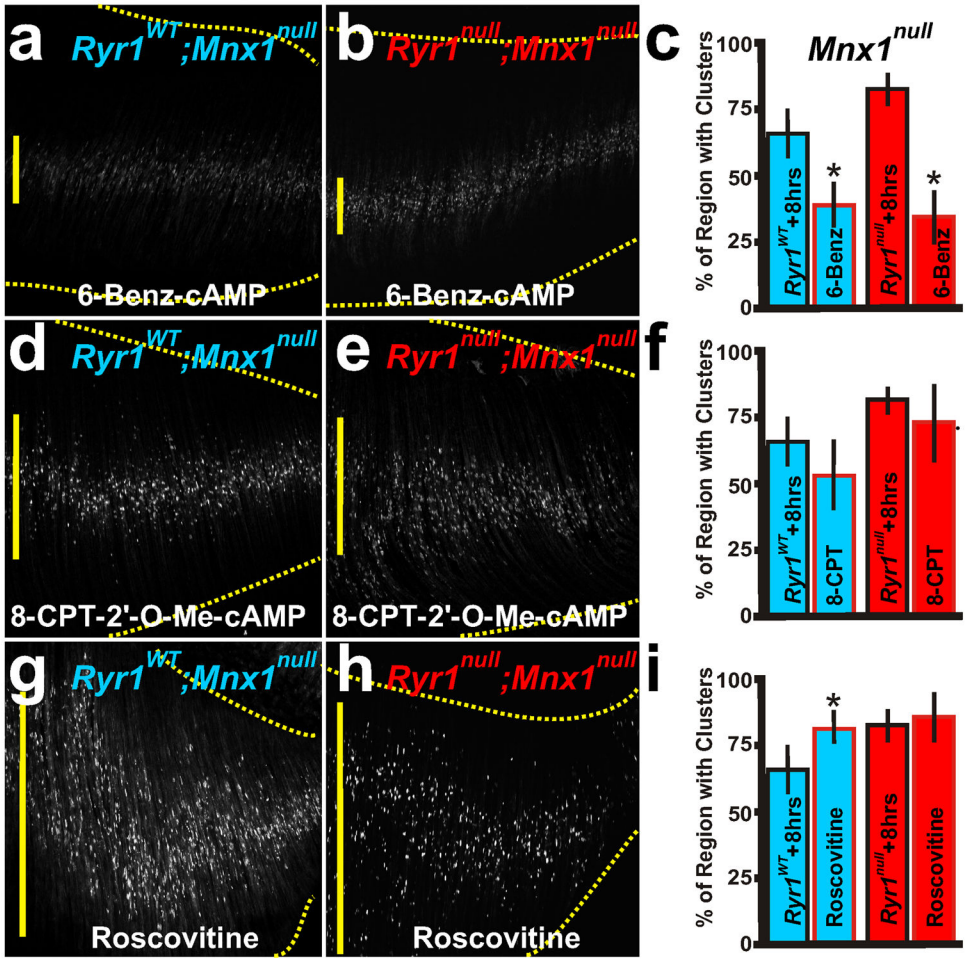

Figure 6.

Intrinsic mechanisms of redistribution of AChR clusters. PKA activation by 6-Benz cAMP (**a–c)** narrowed the AChR cluster patterns in *RyR1*^{null}*; Mnx1*^{null} (**b,c**) similar to *RyR1*^{WT}*; Mnx1*^{null} (**a,c**) explant cultures, whereas cAMP (EPAC) activation by 8-CPT-2′-O-Me cAMP did not (**d–f). g–i,** Inhibition of CDK5 activity by roscovitine expanded the patterned region in *RyR1*^{WT}*; Mnx1*^{null} explants (**g**), to a region more similar to that of *RyR1*^{null}*; Mnx1*^{null} explants. Asterisks show significance ($p<0.05$) of samples to explant controls of *RyR1*^{WT} and *RyR1*^{null}. Scale bar = 200 μm; yellow vertical line represents the largest width of the AChR cluster region within ventral quadrant of diaphragm shown. Red outline in **c, f, i** indicate drug treatment. Each condition was performed in 5 diaphragms.

Table 1

Average number of AChR clusters per 100μm between the most distal α-bungarotoxin positive AChR clusters

	Mnx1^{WT}	**Mnx1^{null}**
Fresh-fixed Diaphragm	34+/−5	48+/−5
8 hr Diaphragm explant	37+/−6	46+/−9
Stim 5.6 mHz	31+/−9	18+/−11*
Stim 1.7mHz	39+/−11	25+/−10*
Wnt3a	40+/−10	38+/−9
Wnt3a +Nitrend.	36+/−6	8+/−2*
Wnt3a +*RyR1^{null}*	22+/−3*	3+/−1*
RyR1^{null}	43+/−7	48+/−8
Stim 5.6 mHz +*RyR1^{null}*	22+/−5*	6+/−4*
NRG1	42+/−10	25+/−6*
NRG1 +*RyR1^{null}*	39+/−7	28+/−4*
Agrin	43+/−10	44+/−13
Agrin +*RyR1^{null}*	84+/−14*	97+/−21*
6-Benz cAMP	41+/−11	44+/−14
6-Benz cAMP +*RyR1^{null}*	42+/−14	48+/−8
8-CPT-2′-O-Me cAMP	35+/−14	44+/−13
8-CPT-2′-O-Me +*RyR1^{null}*	32+/−14	31+/−9
Roscovitine	43+/−10	47+/−10
Roscovitine +*RyR1^{null}*	39+/−14	48+/−11

Average value from 5 diaphragm explants. Asterisks indicates $p<0.005$ (SEM)